Absolute partial cross sections for electron-impact ionization of H2O and D2O from threshold to 1000 eV

H. C. Straub, B. G. Lindsay, K. A. Smith, and R. F. Stebbings

Additional information on J. Chem. Phys.

Absolute partial cross sections for electron-impact ionization of H_2O and D_2O from threshold to 1000 eV

H. C. Straub, B. G. Lindsay,[a] K. A. Smith, and R. F. Stebbings

Department of Space Physics and Astronomy, Department of Physics, and Rice Quantum Institute, Rice University, 6100 Main Street, Houston, Texas 77005-1892

Absolute partial cross sections for electron-impact ionization of H_2O and D_2O are reported for electron energies from threshold to 1000 eV. Data are presented for the production of $H_2O^+ + OH^+ + O^+$, O^{2+}, H_2^+, and H^+ from H_2O and for the production of D_2O^+, OD^+, O^+, O^{2+}, D_2^+, and D^+ from D_2O. The product ions are mass analyzed using a time-of-flight mass spectrometer and detected with a position-sensitive detector whose output demonstrates that all product ions are completely collected. The overall uncertainty in the absolute cross section values is $\pm 4.5\%$ for singly charged parent ions and is slightly greater for fragment ions. The cross sections for H_2O and D_2O are found to be the same to within experimental uncertainties except for the H_2^+ cross section which is approximately a factor of 2 greater than the D_2^+ cross section. Previous results are compared to the present measurements. © *1998 American Institute of Physics.*
[S0021-9606(98)01201-X]

I. INTRODUCTION

Cross sections for electron-impact ionization of water vapor are important, among other things, for understanding the physics and chemistry of planetary atmospheres. There have been several previous studies of electron-impact ionization of water vapor; however, the agreement among them is poor. Cracking patterns for H_2O were measured by Mann, Hustrulid, and Tate[1] and by Rudolph and Melton.[2] Total cross sections for H_2O were measured by Schutten *et al.*[3] and by Bolorizadeh and Rudd[4] while Djurić, Čadež, and Kurepa[5] measured total cross sections for both H_2O and D_2O. Partial cross sections for H_2O have been measured by Gomet,[6] by Orient and Srivastava,[7] and Rao, Iga, and Srivastava.[8] Märk and Egger[9] measured cross sections for single ionization of the parent species for both H_2O and D_2O. Partial cross sections for H_2O were calculated by Khare and Meath,[10] partial cross sections for dissociative ionization of H_2O were calculated by Khare, Prakash, and Meath,[11] and the total cross section for H_2O was calculated by Hwang, Kim, and Rudd.[12]

This article reports absolute partial cross sections for electron-impact ionization of H_2O and D_2O for electron energies from threshold to 1000 eV. The apparatus and technique used allow each partial cross section to be determined absolutely through direct measurement of all the quantities needed for its evaluation. The results are obtained using a time-of-flight mass spectrometer in which the mass analyzed ions are detected with a position-sensitive detector whose output demonstrates that all product ions, regardless of their initial kinetic energy, are completely collected. The partial cross sections measured are for the production of $H_2O^+ + OH^+ + O^+$, O^{2+}, H_2^+, and H^+ from H_2O and for the production of D_2O^+, OD^+, O^+, O^{2+}, D_2^+, and D^+ from D_2O for electron energies from threshold to 1000 eV. Only the sum of the cross sections for H_2O^+, OH^+, and O^+ are pre-

sented for H_2O since these three ions could not be separately resolved by the mass spectrometer. D_2O is studied in order to provide better separation of the product ions in the mass spectrometer.

II. APPARATUS AND EXPERIMENTAL METHOD

The apparatus shown in Fig. 1 consists of an electron gun, a time-of-flight mass spectrometer with a position-sensitive detector (PSD), and an absolute pressure gauge (not shown). It has been described in detail previously.[13,14] Briefly, during a cross-section measurement the entire vacuum chamber is filled with water vapor at a pressure of approximately 4×10^{-6} Torr. The electron gun produces 20-ns-long pulses, each containing approximately 2500 electrons, at a repetition rate of 2.5 kHz. These pulses are directed through an interaction region, located between two plates maintained at ground potential, and are collected in a Faraday cup. Approximately 200 ns after each electron pulse, a 480 V/cm electric field is applied across the interaction region to drive any positive ions formed by electron impact toward the bottom plate. This electric field is generated by applying a 3 kV pulse with a 55 ns rise time to the top plate. Some ions pass through a grid-covered aperture, 1.91 cm in length in the direction parallel to the electron beam, in the bottom plate. These ions are then accelerated to an energy of 5.4 keV and subsequently impact a PSD, comprising a pair of 25-mm-diameter microchannel plates and a resistive-encoded anode,[15] which records their arrival times and positions. The ion arrival times are used to identify their mass-to-charge ratios and the ion arrival positions are used to determine the effectiveness of product ion collection.

Under conditions in which very few of the incident electrons produce an ion, the partial cross section $\sigma(X)$ for production of ion species X is given by

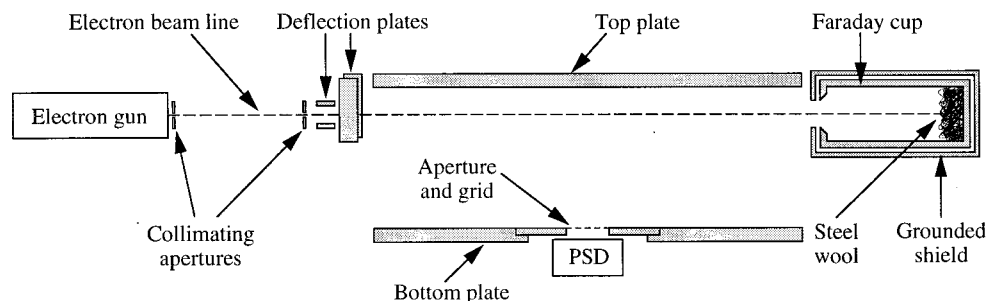[a]Electronic mail: lindsay@ruf.rice.edu

FIG. 1. Schematic diagram of the apparatus.

$$\sigma(X) = \frac{N_i(X)}{N_e n l}, \qquad (1)$$

where $N_i(X)$ is the number of X ions produced by a number N_e of electrons passing a distance l through a uniform water vapor target of number density n. Determination of an absolute cross section requires measurement of all four quantities
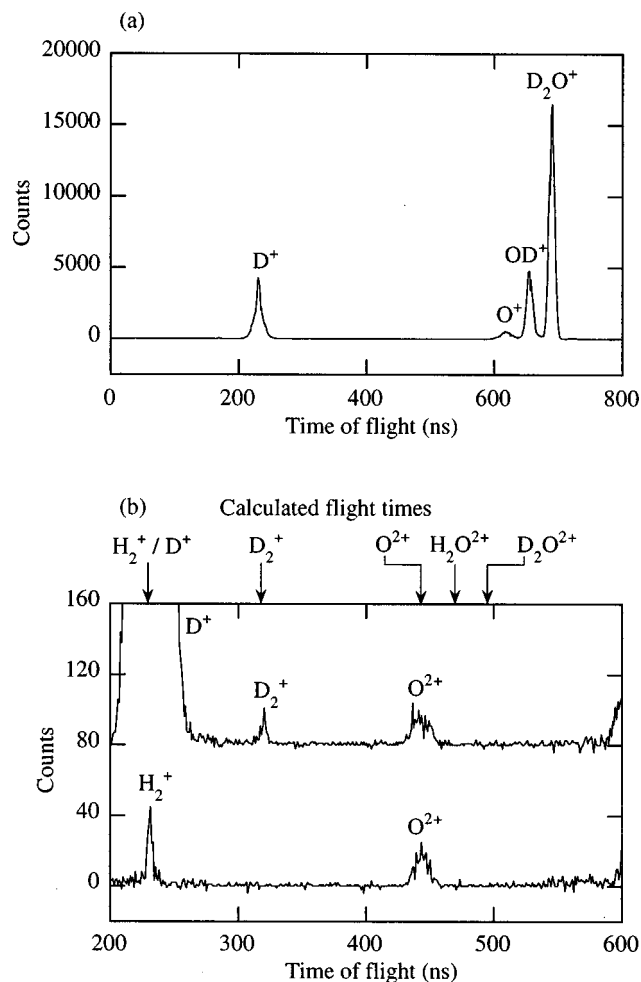

FIG. 2. (a) Time-of-flight spectrum for ions produced by 200 eV electron impact on D_2O. (b) Portions of the time-of-flight spectrums for 200 eV electron impact on H_2O and D_2O. The lower spectrum is for H_2O and the upper spectrum, which has been shifted upward by 80 counts, is for D_2O. Calculated flight times for H_2^+, D^+, D_2^+, O^{2+}, H_2O^{2+}, and D_2O^{2+} are also indicated.

on the right-hand side of Eq. (1) and has been previously described in detail.[13,14] Briefly, the number of electrons N_e is determined by collecting the electron beam in a Faraday cup and measuring the current with an electrometer operating in the charge collection mode. Measurement of $N_i(X)$ is accomplished by recording the time-of-flight spectrum, counting the number ions in an appropriate portion of the spectrum, and accounting for the detection efficiency for the combination of grid and PSD. This detection efficiency was determined to be $(37.8 \pm 0.2)\%$ and to be independent of ion species by repetitively directing an ion beam of appropriate species and energy alternately onto the PSD and into a second Faraday cup (not shown in Fig. 1). The effective path length l from which detected ions originate is accurately given by the 1.91 cm length of the aperture directly in front of the PSD.[14] The target number density n is obtained from measurements of the gas pressure using a capacitance diaphragm gauge.[16]

Determination of the gas pressure is more difficult for water vapor than it was for gases used in previous work[13,14] with this apparatus. When working with gases such as N_2 and O_2, the pressure measured by the capacitance diaphragm gauge comes to equilibrium in a few seconds; however, for H_2O and D_2O it requires approximately 5 min for the pressure reading to achieve equilibrium. Accurate pressure measurement with the capacitance diaphragm gauge at pressures of 4×10^{-6} Torr requires frequently removing gas from the vacuum chamber and checking the zero reading of the gauge in order to compensate for drift of its zero reading. The additional waiting time required after adding or removing H_2O and D_2O from the vacuum chamber increases the statistical uncertainty of the pressure measurement from $\pm 2.5\%$ in previous work to $\pm 3.5\%$ in the present experiment.

For the H_2O cross-section measurements, de-ionized water was used. It was thoroughly degassed prior to use and contamination of H_2O by other gases was observed to be less than 0.1%. The D_2O was obtained from Aldrich Chemical Company with a specified minimum isotopic purity for the deuterium of 99.98% and was also degassed prior to use. The isotopic purity of the D_2O could be checked by comparing the counts in the H^+ and D^+ peaks after appropriate subtraction of the background gas signal. The isotopic purity initially observed for deuterium was only 95% with the H^+ impurity coming principally from HDO. However, if D_2O was admitted to the chamber at a pressure of 3×10^{-5} Torr
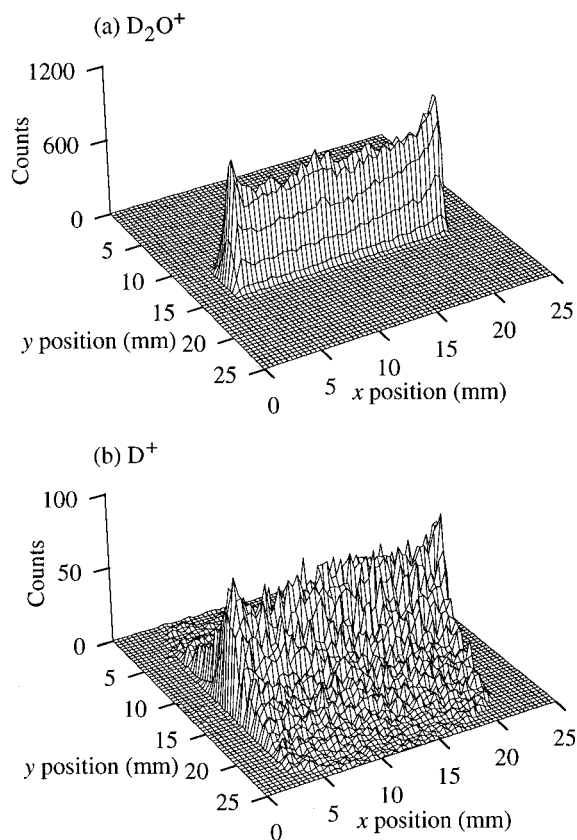
FIG. 3. Arrival position distribution for (a) D$_2$O$^+$ and (b) D$^+$ ions produced by 100 eV electron impact on D$_2$O. The electron beam is parallel to the x direction.

FIG. 4. Position and time-of-flight distribution produced by 200 eV electron impact on (a) D$_2$O and (b) H$_2$O. Note that the tops of the D$_2$O$^+$, OD$^+$, H$_2$O$^+$, and OH$^+$ peaks have been cut off in order to provide more detail for the O$^+$, D$^+$, and H$^+$ peaks. The D$_2$O$^+$, OD$^+$, H$_2$O$^+$, and OH$^+$ peaks actually extend up to 50 000, 11 500, 59 000, and 11 500 counts, respectively.

for 24 h prior to taking data, the observed isotopic purity for deuterium increased to better than 99.5% and the background gas was seen to change from primarily H$_2$O to a mixture of H$_2$O, HDO, and D$_2$O. Therefore, whenever data were not being taken, D$_2$O was admitted to the chamber at a pressure of 3×10^{-5} Torr to ensure good isotopic purity.

A typical time-of-flight spectrum for D$_2$O is shown in Fig. 2(a) which demonstrates the mass resolution of the apparatus. As can be seen in Fig. 2(a), the D$_2$O$^+$, OD$^+$, and O$^+$ peaks are not completely resolved, however, it is estimated that the slight overlap causes an error in the cross section determination of not more than 0.5%, 1.5%, and 4% for the D$_2$O$^+$, OD$^+$, and O$^+$ cross sections, respectively. Figure 2(b) shows portions of the time-of-flight spectra of H$_2$O and D$_2$O in the vicinity of the O^{2+} peak. The calculated flight times for O^{2+}, H$_2$O^{2+}, and D$_2$O^{2+} are marked. Cross sections for H$_2$O^{2+} have been previously reported,[8] however, no evidence for this ion or for D$_2$O^{2+} is seen in the present experiment.

The ion arrival position distributions for D$_2$O$^+$ and D$^+$ are shown in Fig. 3. The D$_2$O$^+$ parent ions, which are formed with thermal energy, impact on a narrow strip located immediately beneath the electron beam while the energetic D$^+$ fragment ions are detected over a much wider area of the PSD. From the arrival position distributions, it is determined that all product ions for both H$_2$O and D$_2$O are completely collected. The position distributions are truncated at approxi-
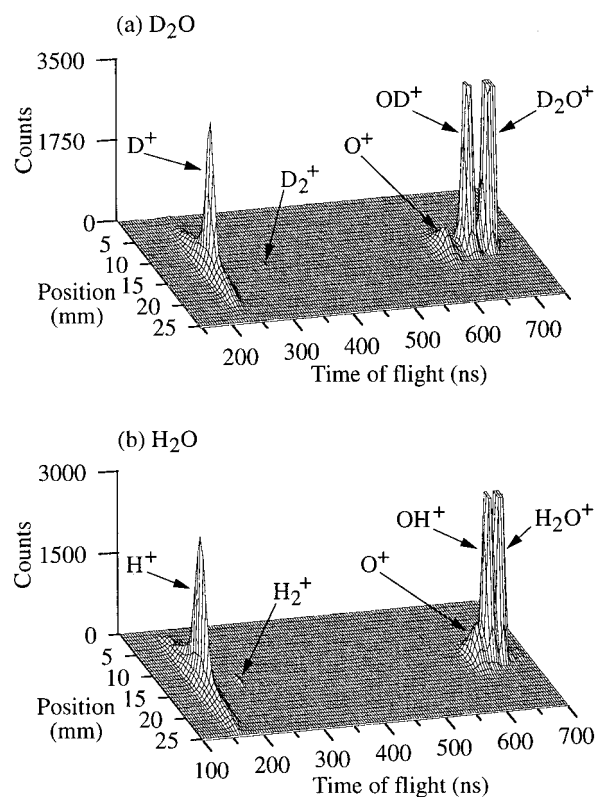
mately 3 and 22 mm on the x axis due to the aperture immediately in the front of the PSD. The enhanced signals seen at the ends of the position distributions are due to a slight focusing of the ions' trajectories that occurs during their acceleration toward the PSD after they pass through the grid-covered aperture. The effective path length from which detected ions originate is therefore still equal to the length of the aperture.

Figure 4 shows plots for H$_2$O and D$_2$O in which the ions' transverse arrival positions at the PSD (i.e., the displacement of ions perpendicular to the electron beam axis) have been combined with their flight times. As can be seen, the mass resolution of the D$_2$O product ions is superior to that for the H$_2$O product ions. For H$_2$O, only the sum of the cross sections for H$_2$O$^+$, OH$^+$, and O$^+$ may be determined accurately. The widths in both position and time of the singly ionized parent molecule peaks are due to the spatial extent of the electron beam while the greater widths for the fragment ion peaks are due to the fragment ions' initial velocities perpendicular to the electron beam in addition to the spatial extent of the electron beam. Even the most energetic ions, H$^+$ from H$_2$O and D$^+$ from D$_2$O, are seen to be completely collected.

TABLE I. Ion counting statistics and the relative and absolute uncertainties associated with the partial cross sections for H_2O and D_2O. The ion counting statistics represent one standard deviation. The uncertainties for σ(total) come from an appropriately weighted sum of the uncertainties for the partial cross sections.

Target	Cross section	Ion counting statistics (%)	Relative uncertainty (%)	Absolute uncertainty at 100 eV (%)	Absolute uncertainty at all other energies (%)
H_2O	$\sigma(H_2O^++OH^++O^+)$	0.5	± 2.0	± 4.0	± 4.5
	$\sigma(O^{2+})$	7.5	± 8.0	± 8.5	± 11.5
	$\sigma(H_2^+)$	7.5	± 8.0	± 8.5	± 11.5
	$\sigma(H^+)$	1.5	± 2.5	± 4.5	± 5.0
	σ(total)		± 2.0	± 4.0	± 4.5
D_2O	$\sigma(D_2O^+)$	0.5	± 2.0	± 4.0	± 4.5
	$\sigma(OD^+)$	1.5	± 3.0	± 4.5	± 5.5
	$\sigma(O^+)$	2.5	± 5.0	± 6.0	± 8.0
	$\sigma(O^{2+})$	7.5	± 8.0	± 8.5	± 11.5
	$\sigma(D_2^+)$	10.0	± 10.5	± 11.0	± 15.0
	$\sigma(D^+)$	1.5	± 2.5	± 4.5	± 5.0
	σ(total)		± 2.0	± 4.0	± 4.5

III. CROSS SECTION DETERMINATION AND UNCERTAINTIES

Measurement of all the quantities on the right-hand side of Eq. (1) allows direct determination of absolute partial cross sections. Since pressure measurements using the capacitance diaphragm gauge that are needed for determination of the number density n are extremely time consuming, absolute measurement of the cross sections was made at an electron energy of 100 eV, and the relative shapes of the partial cross sections were determined by measuring the cross sections at various energies relative to the cross section at 100 eV. Absolute H_2O and D_2O cross sections were measured for gas pressures between 10^{-6} and 10^{-5} Torr and found to be invariant with respect to the pressure.

A detailed analysis of the experimental uncertainties has been given previously.[13] Table I gives the ion counting statistics and the relative and absolute uncertainties for all cross sections measured in this work. The relative uncertainties come from the ion counting statistics, the uncertainties (given in Sec. II) due to incomplete separation of the D_2O^+, OD^+, O^+ peaks for D_2O, and a $\pm 0.5\%$ uncertainty in the electron beam current measurement. The absolute uncertainties in the cross sections come from the ion counting statistics, the uncertainties (given in Sec. II) due to incomplete separation of the D_2O^+, OD^+, O^+ peaks for D_2O, a $\pm 0.5\%$ uncertainty associated with determination of the detection efficiency, a $\pm 0.5\%$ uncertainty in the electron beam current measurement, a $\pm 0.5\%$ uncertainty in the calibration of the electrometer used for the electron beam current measurement and PSD detection efficiency determination, a $\pm 1\%$ uncertainty in the target length, a $\pm 3.5\%$ statistical uncertainty and a $\pm 1\%$ calibration uncertainty in the pressure measurement with the capacitance diaphragm gauge, and a $\pm 0.2\%$ uncertainty in the temperature measurement needed for calculation of the number density. The energy of the electron beam was established to better than ± 1 eV by observing the threshold for He^+ formation.

IV. RESULTS AND DISCUSSION

The measured absolute partial cross sections for H_2O and D_2O are listed in Tables II and III and are plotted in Figs. 5–11. The total cross sections shown in Fig. 5 are the sum of the measured partial cross sections. Except for the H_2^+

TABLE II. Present results for the partial cross sections of H_2O.

Electron energy (eV)	$\sigma(H_2O^++OH^++O^+)$ $(10^{-16}$ cm$^2)$	$\sigma(O^{2+})$ $(10^{-19}$ cm$^2)$	$\sigma(H_2^+)$ $(10^{-19}$ cm$^2)$	$\sigma(H^+)$ $(10^{-17}$ cm$^2)$
13.5	0.034			
15	0.133			
17.5	0.292			
20	0.457			0.026
22.5	0.628			0.098
25	0.779			0.223
30	1.04		0.30	0.465
35	1.24		0.78	0.813
40	1.41		1.31	1.18
45	1.52		1.53	1.55
50	1.61		1.55	1.90
60	1.74		1.66	2.50
70	1.80		1.70	2.95
80	1.85		1.70	3.35
90	1.86	0.08	1.75	3.62
100	1.87	0.20	1.75	3.80
110	1.86	0.48	1.73	3.90
125	1.82	0.72	1.66	3.94
150	1.76	1.22	1.62	3.89
175	1.69	1.85	1.56	3.83
200	1.64	1.87	1.56	3.65
250	1.49	2.03	1.38	3.28
300	1.35	1.85	1.35	2.94
400	1.17	1.38	1.27	2.44
500	0.999	1.08	0.91	2.04
600	0.884	0.99	0.95	1.76
700	0.779	0.82	0.61	1.52
800	0.709	0.81	0.74	1.37
900	0.653	0.61	0.72	1.22
1000	0.595	0.67	0.57	1.11

TABLE III. Present results for the partial cross sections of D$_2$O.

Electron energy (eV)	$\sigma(D_2O^+)$ (10^{-16} cm^2)	$\sigma(OD^+)$ (10^{-17} cm^2)	$\sigma(O^+)$ (10^{-18} cm^2)	$\sigma(O^{2+})$ (10^{-19} cm^2)	$\sigma(D_2^+)$ (10^{-19} cm^2)	$\sigma(D^+)$ (10^{-17} cm^2)
13.5	0.028					
15	0.136					
17.5	0.295	0.014				
20	0.444	0.157				0.020
22.5	0.593	0.540				0.097
25	0.703	0.921	0.24			0.200
30	0.875	1.72	0.39		0.20	0.469
35	1.03	2.38	0.75		0.42	0.757
40	1.12	2.83	1.41		0.61	1.12
45	1.20	3.20	2.21		0.75	1.47
50	1.26	3.51	2.93		0.69	1.80
60	1.32	3.87	4.18		0.70	2.40
70	1.35	4.13	5.13		0.73	2.86
80	1.38	4.32	6.28		0.67	3.28
90	1.38	4.35	7.03	0.12	0.83	3.49
100	1.38	4.41	7.32	0.27	0.79	3.68
110	1.36	4.36	7.76	0.55	0.77	3.78
125	1.33	4.32	8.02	0.72	0.68	3.82
150	1.27	4.11	7.87	1.01	0.81	3.73
175	1.21	3.98	7.64	1.58	0.74	3.64
200	1.17	3.79	7.37	1.75	0.57	3.48
250	1.05	3.47	6.58	1.72	0.52	3.13
300	0.954	3.22	5.71	1.70	0.47	2.78
400	0.814	2.74	4.47	1.26	0.42	2.28
500	0.715	2.37	3.83	1.15	0.33	1.93
600	0.632	2.08	3.20	0.86	0.30	1.65
700	0.566	1.89	2.77	0.78	0.34	1.48
800	0.512	1.72	2.44	0.60	0.23	1.30
900	0.473	1.59	2.24	0.64	0.33	1.18
1000	0.438	1.46	1.97	0.53	0.25	1.10

cross section, all of the H$_2$O cross sections are in good agreement with the D$_2$O cross sections. The H$^+$ cross section is consistently larger than the D$^+$ cross section; however, the magnitude of the difference ($\sim$5%) is within the experimental uncertainties. This is consistent with the work of Märk and Egger[9] who found the cross sections for single ionization of the parent species to be the same to within uncertainties for H$_2$O and D$_2$O and the work of Djurić, Čadež, and Kurepa[5] who found that the H$_2$O and D$_2$O total cross sec-

FIG. 5. Present results for the D$_2$O total cross section (●), the H$_2$O total cross section (–), the D$_2$O$^+$+OD$^+$+O$^+$ cross section (○), and the H$_2$O$^+$+OH$^+$+O$^+$ cross section (- - -).

tions agreed to within uncertainties. Due to the good agreement between the H$_2$O$^+$+OH$^+$+O$^+$ and D$_2$O$^+$+OD$^+$+O$^+$ cross sections, the cross sections for H$_2$O$^+$, OH$^+$, and O$^+$ from H$_2$O, which could not be individually determined due to their poor separation in the mass spectrometer, should be equivalent within experimental uncertainties to the measured cross sections for D$_2$O$^+$, OD$^+$, and O$^+$ from D$_2$O.

The H$_2^+$ cross section is approximately a factor of 2 greater than the D$_2^+$ cross section and this difference is significantly larger than the experimental uncertainties. One interesting point to note is that if the water vapor cross sections are measured while an ionization gauge is on, the H$_2^+$ and D$_2^+$ cross sections are each found to be a factor of 2 larger than with the ionization gauge off. The remaining partial cross sections of H$_2$O and D$_2$O are found to be identical whether or not the ionization gauge is on. The cross sections presented in Tables II and III were all taken with the ionization gauge off. Presumably a small fraction ($\sim$0.1%) of the H$_2$O or D$_2$O is converted to H$_2$ or D$_2$ by the hot thoriated iridium filament of the ionization gauge and the large cross sections for production of H$_2^+$ from H$_2$ and for production of D$_2^+$ from D$_2$ causes the apparent increase in the H$_2^+$ from H$_2$O and D$_2^+$ from D$_2$O cross sections. With the ionization gauge on, the threshold for H$_2^+$ and D$_2^+$ formation is observed to be less than 20 eV while it is found to be between 25 and 30 eV with the ionization gauge off. Mann, Hustrulid, and Tate[1]
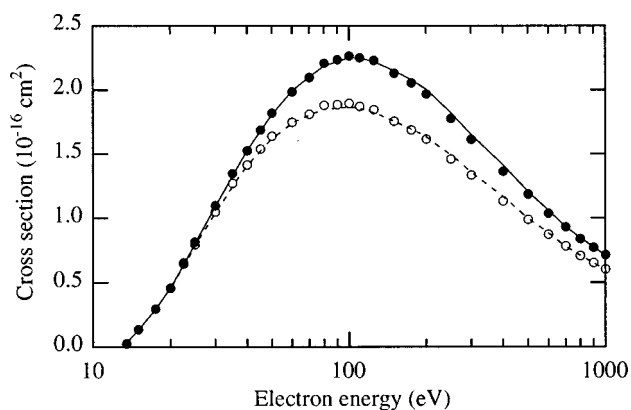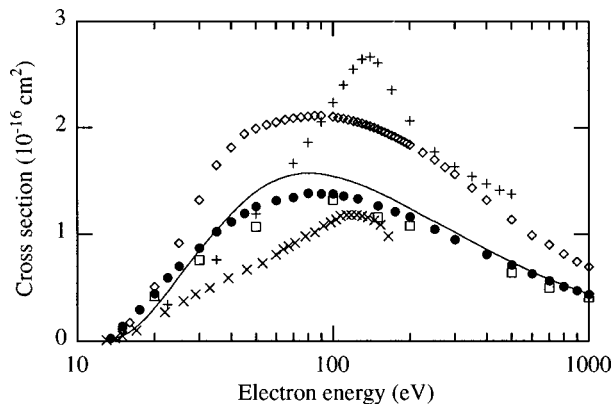
FIG. 6. D$_2$O$^+$ from D$_2$O cross section: present result (●). H$_2$O$^+$ from H$_2$O cross section: Rao, Iga, and Srivastava (Ref. 8) (◇); Märk and Egger (Ref. 9) (×); Gomet (Ref. 6) (+); Schutten *et al.* (Ref. 3) (□); and Khare and Meath (Ref. 10) (–).

FIG. 8. O$^+$ from D$_2$O cross section: present result (●). O$^+$ from H$_2$O cross section: Rao, Iga, and Srivastava (Ref. 8) (◇); Gomet (Ref. 6) (+); Schutten *et al.* (Ref. 3) (□); and Khare, Prakash, and Meath (Ref. 11) (—).

observed the same effect for a tungsten filament and found the threshold for H$_2^+$ from H$_2$O to be 23 ± 2 eV when the water vapor did not come into contact with a hot filament. In the present experiment, there is still a hot filament associated with the indirectly heated cathode of the electron gun, but it has a smaller surface area and operates at a lower temperature than the filament of the ionization gauge. Given the reasonable thresholds for production of H$_2^+$ and D$_2^+$ observed in the present experiment with the ionization gauge off, the cross sections for H$_2^+$ and D$_2^+$ appear to be correct and the large differences between them real.

The measured absolute partial cross sections for H$_2$O and D$_2$O are shown in Figs. 6–11 together with previously published partial cross sections for H$_2$O. The uncertainties in the present partial cross sections are given in Table I while the uncertainties in previous measurements are typically $\pm 10\%$ to $\pm 25\%$. The results of Schutten *et al.*,[3] Gomet,[6] Märk and Egger,[9] and Rao, Iga, and Srivastava[8] are experimental measurements while Khare and Meath[10] calculated partial cross sections for H$_2$O and Khare, Prakash, and Meath[11] recalculated the partial cross sections for
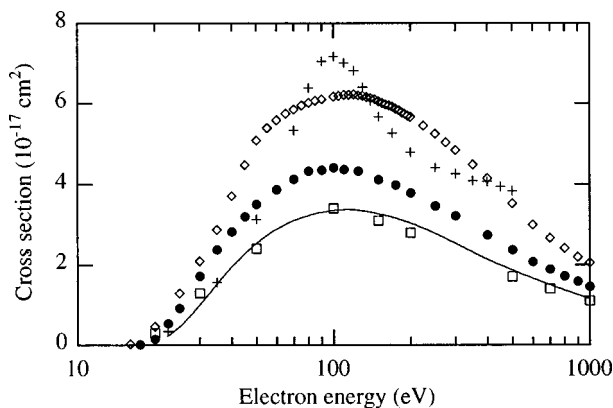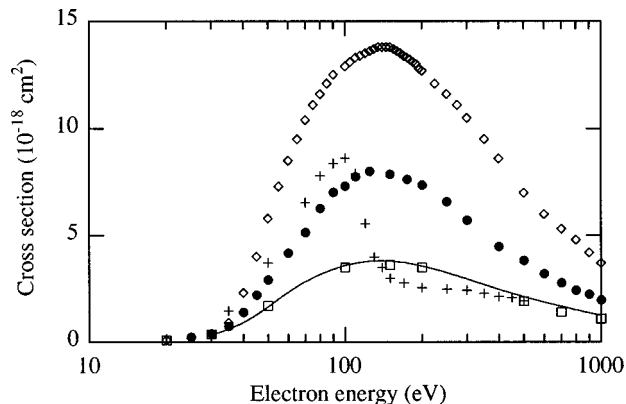
dissociative ionization of H$_2$O. The D$_2$O$^+$ cross section measured by Märk and Egger[9] is not shown since it agrees well with their H$_2$O result and the measurements of Orient and Srivastava[7] are not shown since they have been supplanted by the work of Iga, Rao, and Srivastava.[8] The results of Schutten *et al.*[3] are placed on an absolute scale by normalizing to the total water vapor cross section while Märk and Egger[9] and Rao, Iga, and Srivastava[8] place their results on an absolute scale by normalizing to rare gas cross sections.

For the H$_2$O$^+$ and D$_2$O$^+$ cross sections, the results of Schutten *et al.*[3] and Khare and Meath[10] agree well with the present measurement. The result of Iga, Rao, and Srivastava[8] lies higher than the present measurement, the result of Märk and Egger[9] lies lower than the present measurement, and neither agrees with the present measurement to within the combined uncertainties. For H$_2$O$^+$ and all other partial cross sections, the shapes of Gomet's cross sections[6] are inconsistent with those of others presented here and will not be discussed further. For the OH$^+$ and OD$^+$ cross sections, the results of Schutten *et al.*[3] and Khare, Prakash, and Meath[11] lie too low compared to the present measurement while the work of Rao, Iga, and Srivastava[8] lies too high compared to the present measurement. None of the previous O$^+$ cross
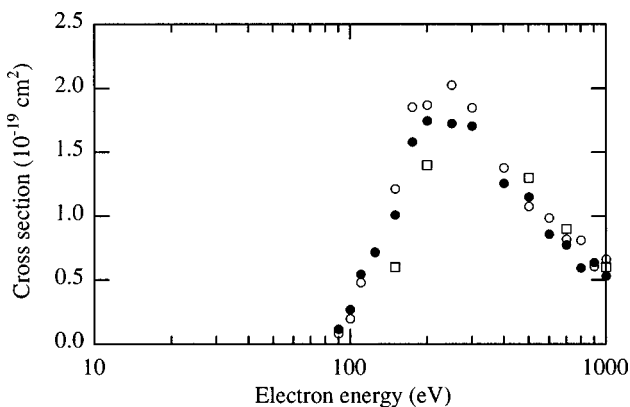
FIG. 7. OD$^+$ from D$_2$O cross section: present result (●). OH$^+$ from H$_2$O cross section: Rao, Iga, and Srivastava (Ref. 8) (◇); Gomet (Ref. 6) (+); Schutten *et al.* (Ref. 3) (□); and Khare, Prakash, and Meath (Ref. 11) (—).

FIG. 9. O^{2+} from D$_2$O cross section: present result (●). O^{2+} from H$_2$O cross section: present result (○) and Schutten *et al.* (Ref. 3) (□).

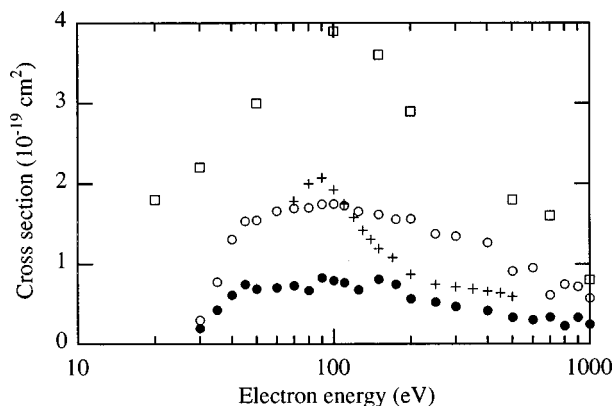FIG. 10. D_2^+ from D_2O cross section: present result (●). H_2^+ from H_2O cross section: present result (○); Gomet (Ref. 6) (+); and Schutten *et al.* (Ref. 3) (□).

FIG. 12. Total cross section for D_2O: present result (●). Total cross section for H_2O: Rao, Iga, and Srivastava (Ref. 8) (◇); Djurić, Čadež, and Kurepa (Ref. 5) (△); Bolorizadeh and Rudd (Ref. 4) (▽); Gomet (Ref. 6) (+); Schutten *et al.* (Ref. 3) (□); Hwang, Kim, and Rudd (Ref. 12) (- - -); and Khare and Meath (Ref. 10) (—).

sections agrees with the present measurement; those of Schutten *et al.*[3] and Khare, Prakash, and Meath[11] lie lower and that of Rao, Iga, and Srivastava[8] lies higher. The O^{2+} measurement of Schutten *et al.*[3] agrees well with the present result. The H_2^+ cross section of Schutten *et al.*[3] lies too high compared to the present result. The work of Schutten *et al.*[3] also has a threshold for H_2^+ formation of less than 20 eV which is probably attributable to a small amount of H_2 being produced in their vacuum chamber by water vapor coming into contact with a hot filament. For the H^+ and D^+ cross sections, the result of Schutten *et al.*[3] agrees well with the present work while the results of Rao, Iga, and Srivastava[8] and Khare, Prakash, and Meath[11] are low compared to the present work.

Rao, Iga, and Srivastava[8] reported observation of the production of H_2O^{2+} from H_2O with a measured cross section of 1.2×10^{-19} cm^2 at an electron energy of 200 eV. As discussed previously, no evidence for this ion was seen in the present experiment. From the data shown in Fig. 2(b), the H_2O^{2+} and D_2O^{2+} cross sections are estimated to be less than 10^{-20} cm^2 at an electron energy of 200 eV. Since Rao,

Iga, and Srivastava[8] did not report detection of any O^{2+}, it would seem probable that the ions identified as H_2O^{2+} are actually O^{2+}.

The present total cross section for D_2O is shown in Fig. 12 together with previous total cross section results for H_2O. The total cross sections of Gomet[6] and of Rao, Iga, and Srivastava[8] are obtained from the sum of their measured partial cross sections. Schutten *et al.*[3] and Djurić, Čadež, and Kurepa[5] measured total cross sections directly using parallel-plate apparatuses. The total cross section for D_2O measured by Djurić, Čadež, and Kurepa[5] is not shown since it agrees well with their H_2O result. Bolorizadeh and Rudd[4] measured doubly differential cross sections and then integrated them to obtain the total cross section. Khare and Meath[10] determined the total cross section by summing their calculated partial cross sections while Hwang, Kim, and Rudd[12] calculated the total cross section directly. The results of Schutten *et al.*,[3] Bolorizadeh and Rudd,[4] Djurić, Čadež, and Kurepa,[5] Khare and Meath,[10] and Hwang, Kim, and Rudd[12] agree with the present measurement to within the combined uncertainties. The result of Rao, Iga, and Srivastava[8] lies higher than the present work and does not agree with the present measurement to within the combined uncertainties. The shape of Gomet's cross section[6] is again inconsistent with that of other investigators.

V. CONCLUSION

Measurements of the absolute partial cross sections for H_2O and D_2O have been presented. The apparatus geometry is of simple design embodying a short-path-length time-of-flight mass spectrometer and position-sensitive detection of the product ions which allows the complete collection of energetic fragment ions from dissociative ionization to be unequivocally demonstrated. Additionally, determination of the ions' detection efficiency and direct measurement of the gas pressure using a capacitance diaphragm gauge allows the cross sections to be measured absolutely. To within experimental uncertainties, the measured cross sections for H_2O
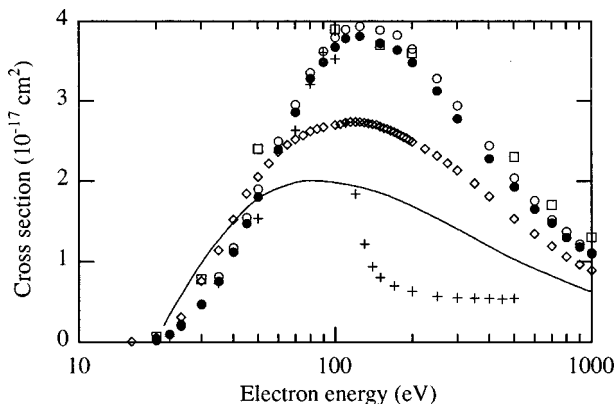

FIG. 11. D^+ from D_2O cross section: present result (●). H^+ from H_2O cross section: present result (○); Rao, Iga, and Srivastava (Ref. 8) (◇); Gomet (Ref. 6) (+); Schutten *et al.* (Ref. 3) (□); and Khare, Prakash, and Meath (Ref. 11) (—).
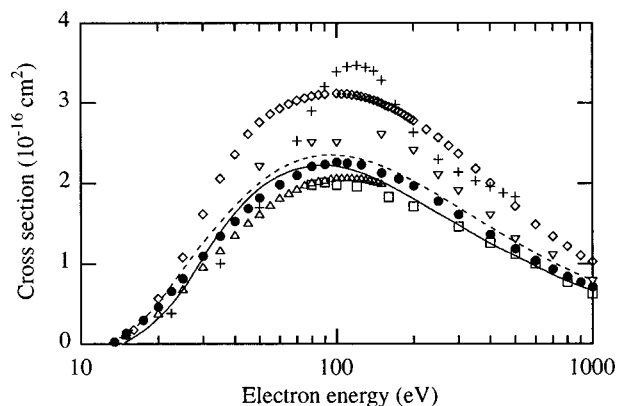
and D_2O were found to be identical except for the H_2^+ cross section which was found to be approximately a factor of 2 greater than the D_2^+ cross section.

ACKNOWLEDGMENTS

[1] M. M. Mann, A. Hustrulid, and J. T. Tate, Phys. Rev. **58**, 340 (1940).

[2] P. S. Rudolph and C. E. Melton, J. Chem. Phys. **45**, 2227 (1966).

[3] J. Schutten, F. J. de Heer, H. R. Moustafa, A. J. H. Boerboom, and J. Kistemaker, J. Chem. Phys. **44**, 3924 (1966).

[4] M. A. Bolorizadeh and M. E. Rudd, Phys. Rev. A **33**, 882 (1986).

[5] N. Lj. Djurić, I. M. Čadež, and M. V. Kurepa, Int. J. Mass Spectrom. Ion Processes **83**, R7 (1988).

[6] J. C. Gomet, C. R. Acad. Sci. Ser. B **281**, 627 (1975).

[7] O. J. Orient and S. K. Srivastava, J. Phys. B **20**, 3923 (1987).

[8] M. V. V. S. Rao, I. Iga, and S. K. Srivastava, J. Geophys. Res. **100**, 26 421 (1995).

[9] T. D. Märk and F. Egger, Int. J. Mass Spectrom. Ion Phys. **20**, 89 (1976).

[10] S. P. Khare and W. J. Meath, J. Phys. B **20**, 2101 (1987).

[11] S. P. Khare, S. Prakash, and W. J. Meath, Int. J. Mass Spectrom. Ion Processes **88**, 299 (1989).

[12] W. Hwang, Y.-K. Kim, and M. E. Rudd, J. Chem. Phys. **104**, 2956 (1996).

[13] H. C. Straub, P. Renault, B. G. Lindsay, K. A. Smith, and R. F. Stebbings, Phys. Rev. A **52**, 1115 (1995).

[14] H. C. Straub, P. Renault, B. G. Lindsay, K. A. Smith, and R. F. Stebbings, Phys. Rev. A **54**, 2146 (1996); H. C. Straub, B. G. Lindsay, K. A. Smith, and R. F. Stebbings, J. Chem. Phys. **105**, 4015 (1996); B. G. Lindsay, H. C. Straub, K. A. Smith, and R. F. Stebbings, J. Geophys. Res. **101**, 21 151 (1996); H. C. Straub, D. Lin, B. G. Lindsay, K. A. Smith, and R. F. Stebbings, J. Chem. Phys. **106**, 4430 (1997).

[15] R. S. Gao, P. S. Gibner, J. H. Newman, K. A. Smith, and R. F. Stebbings, Rev. Sci. Instrum. **55**, 1756 (1984).

[16] H. C. Straub, P. Renault, B. G. Lindsay, K. A. Smith, and R. F. Stebbings, Rev. Sci. Instrum. **65**, 3279 (1994).